Published in final edited form as:
Nat Cell Biol. 2013 June ; 15(6): 647–658. doi:10.1038/ncb2718.

TFEB controls cellular lipid metabolism through a starvation-induced autoregulatory loop

Carmine Settembre[1,2,3,4,*], **Rossella De Cegli**[1,#], **Gelsomina Mansueto**[1,#], **Pradip K. Saha**[5,#], **Francesco Vetrini**[2,3,#], **Orane Visvikis**[6,#], **Tuong Huynh**[2,3], **Annamaria Carissimo**[1], **Donna Palmer**[2], **Tiemo Jürgen Klisch**[2,3], **Amanda C. Wollenberg**[6], **Diego Di Bernardo**[1,7], **Lawrence Chan**[5,8,9], **Javier E. Irazoqui**[6], and **Andrea Ballabio**[1,2,3,4,*]

[1]Telethon Institute of Genetics and Medicine (TIGEM), Via Pietro Castellino 111, 80131, Naples, Italy

[2]Department of Molecular and Human Genetics, Baylor College of Medicine, Houston, Texas, USA

[3]Jan and Dan Duncan Neurological Research Institute, Texas Children Hospital, Houston, Texas, USA

[4]Medical Genetics, Department of Pediatrics, Federico II University, Via Pansini 5, 80131 Naples, Italy

[5]Diabetes and Endocrinology Research Center, Division of Diabetes, Endocrinology and Metabolism, Department of Medicine, Baylor College of Medicine, Houston, Texas, USA

[6]Program in Developmental Immunology, Department of Pediatrics, Massachusetts General Hospital, Harvard Medical School, Boston, Massachusetts, USA

[7]Department of Systems and Computer Science, “Federico II” University of Naples, Naples, Italy

[8]Departments of Molecular & Cellular Biology and Biochemistry, Baylor College of Medicine

[9]St. Luke’s Episcopal Hospital, Houston, Texas, USA

Abstract

The lysosomal-autophagic pathway is activated by starvation and plays an important role in both cellular clearance and lipid catabolism. However, the transcriptional regulation of this pathway in response to metabolic cues is currently uncharacterized. Here we show that the transcription factor EB (TFEB), a master regulator of lysosomal biogenesis and autophagy, is induced by starvation through an autoregulatory feedback loop and exerts a global transcriptional control on lipid catabolism via *PGC1 α* and *PPAR α*. Thus, during starvation a transcriptional mechanism links the autophagic pathway to cellular energy metabolism. The conservation of this mechanism in *Caenorhabditis elegans* suggests a fundamental role for TFEB in the evolution of the adaptive response to food deprivation. Viral delivery of TFEB to the liver prevented weight gain and

[*]Correspondence to: Andrea Ballabio (ballabio@tigem.it) and Carmine Settembre (settembre@tigem.it).
[#]These authors contributed equally and are listed in alphabetical order

Supplementary Information is linked to the online version of the paper. www.nature.com/nature.

Author Contributions C.S., G.M, P.K.S., F.V., O.V., T.H., R.DC., A.C., D.P., T.J.K, A.C.W. performed the experiments. D.d.B. supervised bioinformatic analyses. J.E.I supervised the *C. elegans* experiments, L.C supervised the metabolic studies, A.B. and C.S. designed the overall study and supervised the work. All authors discussed the results and made substantial contributions to the manuscript.

The authors declare no competing financial interests. Readers are welcome to comment on the online version of this article at www.nature.com/nature.

metabolic syndrome in both diet-induced and genetic mouse models of obesity, suggesting a novel therapeutic strategy for disorders of lipid metabolism.

The adaptive response of an organism to food deprivation is associated with major transcriptional and metabolic[1–5] changes and is conserved across evolution[6,7]. One of the most prominent metabolic changes observed during starvation is an increase in lipid catabolism in the liver.

Autophagy, a lysosome-dependent catabolic process, is activated by starvation[8,] and the resulting breakdown products are used to generate new cellular components and energy. Recent studies revealed that autophagy plays a central role in lipid metabolism since it shuttles lipid droplets to the lysosome where they are hydrolyzed into free fatty acids (FFAs) and glycerol[9,10]. Moreover, excessive lipid overload may inhibit autophagy, while enhancing liver autophagy in murine genetic models of obesity (*Ob/Ob*) ameliorates their metabolic phenotype[11]. These observations indicate the close relationship between intracellular lipid metabolism and the lysosomal-autophagic pathway. However, it is not clear how this relationship is coordinated at the transcriptional level in response to environmental cues. Here we show that the basic Helix-Loop-Helix (bHLH) leucine zipper transcription factor TFEB, a master regulator of lysosomal biogenesis and autophagy[12,13] mediates the organismal transcriptional and metabolic responses to starvation.

Starvation induces TFEB expression through an autoregulatory loop

We tested whether starvation activated *TFEB* transcription. *TFEB* expression was significantly induced in liver, muscle, and kidney of mice subjected to 24 hours of food deprivation (Fig. 1a). Similar results were observed *in vivo* using a heterozygous transgenic mouse line (*Tcfeb*-βgal) that carries a *TFEB* gene-trap allele fused with the βgalactosidase gene. In this model we found stronger βgalactosidase staining in the liver and kidney of fasted mice compared to fed mice (Fig. 1b). Starvation time-course studies of HeLa cells, mouse embryonic fibroblasts (MEFs) and hepatocytes revealed a significant and progressive increase of *TFEB* mRNA and protein expression levels starting as soon as 4 hours after the elimination of nutrients from the culture medium (Fig. 1c and Supplementary Fig. 1a). Notably, the cytoplasm-to-nucleus translocation of TFEB[13] occurs at an earlier time point after starvation compared to *TFEB* transcriptional activation (Supplementary Fig. 1b). These observations led us to hypothesize that TFEB exerted a positive effect on its own transcription.

The overexpression of the human *TFEB* cDNA in MEFs from heterozygous *Tcfeb*-βgal transgenic mice resulted in a significant increase in the transcription of the *Tcfeb*–β galactosidase fusion transcript, indicating that the endogenous *TFEB* gene is positively regulated by the exogenous TFEB (Fig. 1d). This result was also confirmed using a set of primers that specifically amplifies the murine endogenous *TFEB* transcript, but does not amplify the exogenous human *TFEB* cDNA (Fig. 1d). These results indicate that exogenous TFEB can induce endogenous *Tcfeb* expression and suggest the presence of a positive feedback loop.

The positive feedback of TFEB on its own expression was significantly enhanced during starvation and was suppressed by re-adding nutrients to the culture medium (Fig. 1e). In addition, the effect of starvation on *TFEB* expression was significantly reduced in MEFs and hepatocytes from heterozygous mice carrying a *Tcfeb*-βgal allele that lacks the transcriptional transactivation domain, indicating that the positive feedback loop requires a functional *TFEB* allele and that TFEB induction by starvation is sensitive to TFEB copy number (Fig. 1f,g).

Next, we tested whether TFEB mediates the positive feedback loop on its own expression by directly binding to its promoter. We previously showed that TFEB recognizes E-box-type DNA sequences, named "CLEAR" motifs[14]. Sequence analysis identified 6 putative CLEAR sites in the promoter region of the *TFEB* gene (Fig. 1h and Supplementary Table 1). Chromatin immunoprecipitation coupled with quantitative PCR (ChIP-qPCR) of liver samples from starved transgenic mice overexpressing a tagged version of TFEB[13] (Supplementary Fig. 2a), showed an enhancement of TFEB binding to CLEAR sites 1, 3,5 and 6 compared to fed controls (Fig. 1h). Thus, *in vitro* and *in vivo* data showed that TFEB controls its own expression by virtue of starvation-induced direct binding to CLEAR elements in the TFEB promoter.

TFEB regulates genes involved in lipid metabolism via *PGC1α* and *PPARα*

To test whether TFEB is in the metabolic response to starvation we sought to define the complete TFEB-dependent transcriptome in the liver, a primary site for the organismal starvation response. To this end, we injected mice with an adenoviral vector that expresses human TFEB (HDAd-*TFEB*) under control of a liver-specific promoter (PEPCK) and with a transgeneless control vector. The levels of expression of TFEB protein under these conditions are shown in Supplementary Fig. 2b. Microarray analysis indicated that as a result of *TFEB* overexpression 773 genes were upregulated and 611 genes were downregulated (GSE35015), using a threshold for statistical significance (FDR<0.05) and further filtering with an absolute Fold Change ≥1.5. Microarray results were validated by quantitative realtime PCR (qRT-PCR) performed on 40 selected genes (Fig. 2a,b). Surprisingly, the gene ontology category[15,16] most significantly up-regulated by *TFEB* overexpression was the cellular lipid metabolic process, which includes monocarboxylic acid, fatty acid, and cellular ketone metabolic processes, among others (Supplementary Table 2). Interestingly, several gene categories related to lipid biosynthesis, such as steroid, lipid and isoprenoid biosynthetic processes were significantly down-regulated (Supplementary Table 3). We also observed that in liver TFEB positively regulates the expression of several genes involved in lysosome organization and autophagy (Supplementary Table 2, Fig. 2b), which is consistent with previous results obtained in cultured cell lines[12–14].

Overall we found that the transcriptional signature of *TFEB* overexpression in liver was similar to that of starvation (GSE36510; Supplementary Table 4), particularly for genes involved in lipid metabolism (Supplementary Fig. 3 and Supplementary Tables 5 and 6). The global control of lipid metabolism exerted by TFEB is illustrated in Fig. 2c and Supplementary Table 7. These results strongly suggested that TFEB overexpression in fed mice phenocopied the transcriptional effects of nutrient deprivation in vivo, supporting the notion that TFEB is a critical regulator of the response to starvation in the liver.

Interestingly, one of the genes whose expression was significantly upregulated following TFEB overexpression was the peroxisome proliferator-activated receptor coactivator 1 *(PGC1)*, a known key regulator of liver lipid metabolism that is transcriptionally induced during starvation[17,18]. To test whether *PGC1 is* a direct target of TFEB we analysed its promoter and identified three CLEAR sites. ChIP-qPCR from liver extracts showed that TFEB binds to two of these sites in a starvation-dependent manner (Fig. 3a). Furthermore, transactivation of a *PGC1 promoter* luciferase reporter by TFEB was dependent on the CLEAR sites (Fig. 3b,c) and was enhanced by starvation (Fig. 3d). These results indicated that TFEB directly regulates *PGC1 gene* expression.

These data were confirmed in vivo by measuring and comparing PGC1 expression in mice that overexpress *TFEB* in the liver and in mice that lack TFEB in the liver (*Tcfeb*-LiKO)

with corresponding control mice. Injection of HDAd-*TFEB* in the liver of fed animals was sufficient to drive high constitutive *PGC1* expression to levels similar as those observed in uninjected starved animals. In contrast, *PGC1* induction by starvation was partially blocked by the deletion of *TFEB.* Furthermore, primary hepatocytes from animals overexpressing *TFEB* showed high constitutive expression of *PGC1* while *TFEB* deletion did not affect basal *PGC1* expression. In contrast, *PGC1* induction was partially blunted in starved hepatocytes lacking TFEB, indicating that starvation induces *PGC1* in a TFEB-dependent manner. In starved hepatocytes overexpression of *TFEB* caused synergistic induction of *PGC1* expression beyond the levels obtained by starvation only (Fig. 3e). Together, these results strongly suggested that TFEB directly controls *PGC1* induction during liver starvation response, and that the level of TFEB expression is a critical parameter for the magnitude of this response.

To study the role of PGC1 as a mediator of TFEB function, we overexpressed TFEB in a mouse line that lacks PGC1 in the liver, which was generated by injecting *PGC1* flox/flox mice with a helper-dependent adenovirus containing the CRE recombinase (HdAD-APOA1-CRE). Fig 3f shows that TFEB-mediated induction of the expression of genes involved in lipid metabolism was severely reduced in the absence of PGC1, confirming that PGC1 acts downstream of TFEB and mediates TFEB function.

During starvation PGC1 regulates lipid metabolism in the liver via the downstream nuclear receptor peroxisome proliferator activated receptor (PPAR)[17,18], suggesting that PGC1 may mediate TFEB function by controlling the activity of PPAR To test this hypothesis, we analyzed transcript levels for known targets of PPAR [17–20] in *Tcfeb*-LiKO mice, compared to wild type mice. Starvation caused induction of the PPAR target genes in wild type mice, but not in *Tcfeb*-LiKO mice (Fig. 3g and Supplementary Fig. 4a), indicating that TFEB is essential for PPAR activation by starvation. Furthermore, the majority (74%) of the genes that were induced by TFEB overexpression in the liver of wild type mice failed to show a transcriptional induction in mice lacking *PPAR* as measured by microarray analysis of liver tissue (GSE41141; Supplementary Table 8), suggesting that PPAR is an important mediator of TFEB transcriptional activity in the liver during starvation.

TFEB regulates lipid breakdown in the liver

Histological analysis of liver samples did not reveal any significant differences between wild type and *Tcfeb*-LiKO mice fed with a normal diet. However, after a 24 h fast we observed an accumulation of lipid droplets in *Tcfeb*-LiKO mice that was not found in wild-type littermates, suggesting a defect in intracellular lipid degradation (Fig. 4a–c). Consistently, we detected an impairment of free fatty acid (FFA) oxidation in cultured hepatocytes (Fig. 4d) and higher levels of circulating FFA (Fig. 4e) and glycerol (Fig. 4f) in *Tcfeb*-LiKO mice compared to controls. In addition, during starvation *Tcfeb*-LiKO mice showed decreased plasma levels of circulating ketone bodies, which are mainly produced in the liver from the oxidation of fatty acids (Fig. 4g). These data demonstrate the importance of TFEB in the control of cellular lipid metabolism. In addition, EchoMRI analysis of whole body compositions demonstrated a defective peripheral fat mobilization after a 24 h and a 48 h fast (Fig. 4h). This observation could explain the increased peripheral adiposity in *Tcfeb*-LiKO mice compared to controls (Fig. 4i), indicating that TFEB activity in liver also affects peripheral fat metabolism.

Next we addressed the role of TFEB in fat storage and its utilization in animals challenged with a high-fat diet. Liver appearance and lipid content were examined in *Tcfeb*-LiKO, HDAd-*TFEB*-injected and in corresponding control mice. Livers from *Tcfeb*-LiKO mice were large, pale, and filled with lipid vacuoles consistent with an impairment of lipid

degradation pathways. Control mice fed with the same diet showed a similar, albeit milder, phenotype, in spite of similar food intake. Conversely, livers from HDAd-*TFEB*-injected mice displayed normal red color, markedly reduced lipid content compared with wild-type controls, and normal weight in spite of increased food intake compared with control mice, suggesting that *TFEB* overexpression prevented the effects of the high-fat diet by enhancing lipid degradation (Fig. 5a–c and Supplementary Fig. 4b).

Blocking autophagy in the liver leads to hepatomegaly and liver failure[21]. Recently, a significant increase of lipid droplets, cholesterol and triglycerides was observed in the liver of Atg7 KO mice, suggesting a role of autophagy in lipid degradation[9]. We analyzed TFEB-mediated lipid degradation in *Atg7* liver-KO mice, in which autophagy is blocked[21]. Liver-specific Atg7 KO mice were generated by injecting Atg7 flox/flox mice with a helper-dependent virus containing the CRE recombinase (HdAD-APOA1-CRE) (Supplementary Fig. 5a). One month after TFEB injection, the mice presented a significant increase in liver size and increased markers of liver damage, as measured by ALT /AST/ALP, which is consistent with previous results[21]. At the cellular level we observed an accumulation of P62[22] (Supplementary Fig. 5b) and lipid droplets (Fig. 5d–f). However, *TFEB* overexpression failed to decrease lipid droplet number (Fig. 5d), liver weight gain (Fig. 5e) and lipid content (Fig. 5f) in Atg7 liver-KO mice (Supplementary Fig. 5b,c), which is in contrast to the results obtained by *TFEB* overexpression in wild type mice (Fig. 5a–c). These results indicate that autophagy is required for TFEB-mediated lipid degradation.

TFEB overexpression rescues obesity and metabolic syndrome in mice

When fed a regular chow diet, HDAd-*TFEB*-injected mice were significantly leaner than controls (Fig. 6a), with decreased body fat deposition (Fig. 6b), in spite of exhibiting similar food intake. Interestingly, these differences were blunted when HDAd-*TFEB* was injected in *PPAR* □KO mice (Fig. 6a,b), consistent with our results showing that PPAR □is required for transcriptional changes downstream of TFEB. HDAd-*TFEB*-injected wild type mice also exhibited lower plasma levels of total cholesterol, triglycerides, VLDL, leptin, insulin and glucose (Fig. 6c–i). Indirect calorimetric analysis revealed a decrease in respiratory exchange rate (RER) (Fig. 6j) and an increase in FFA oxidation rate in HDAd-*TFEB*-injected mice compared with controls (Fig. 6k). Overall, the phenotype observed in HDAd-*TFEB*-injected mice shared some similarities to those reported for mice under caloric restriction[23].

Next we tested the metabolic effects of TFEB gain and loss of function in mice fed with a high-fat diet. We found that in this condition *Tcfeb*-LiKO mice gained substantially more weight than control littermates (Fig. 7a). Conversely, *TFEB* overexpression by injection of HDAd-*TFEB* at the beginning of the high fat diet (“Early inj”) significantly prevented the development of obesity. Furthermore, the injection of HDAd-*TFEB* after 4 weeks of high fat diet (“Late inj”) completely arrested the development of the obese phenotype. In addition, after 10 weeks of high fat diet the weights of the animals injected at the beginning of the experiment and those injected after 4 weeks were indistinguishable (Fig. 7a). Body composition analysis revealed that the weight difference between *Tcfeb*-LiKO and HDAd-*TFEB*-injected mice was largely due to differences in fat accumulation, which was higher in *Tcfeb*-LiKO and lower in HDAd-*TFEB*-injected mice compared with controls (Fig. 7b). Of note, the abnormalities in the serum metabolic profile induced by the high-fat diet in wild type mice, which was characterized by the increase of circulating leptin, insulin, triglycerides, and cholesterol, was markedly attenuated in HDAd-*TFEB*-injected mice (Fig. 7c–f), which also showed improved sugar metabolism, as demonstrated by glucose and insulin-tolerance tests (Fig. 7g–i).

Similar experiments were performed in a genetic model of obesity due to leptin deficiency (*Ob/Ob*), which is associated with hyperphagia[24]. Two-month-old *Ob/Ob* mice, already obese at this early age, were injected with HDAd-*TFEB*. Six weeks later HDAd-*TFEB*-injected *Ob/Ob* mice had significantly reduced levels of circulating triglycerides, cholesterol, glucose and insulin, and an improved glucose tolerance test, compared with untreated *Ob/Ob* mice, indicating that liver overexpression of *TFEB* improved the metabolic syndrome phenotype (Supplementary Fig. 6). Together, these observations demonstrate that high TFEB activity can not only prevent the metabolic syndrome, but also revert it once initiated.

Evolutionary conservation of TFEB regulation and function in *Caenorhabditis elegans*

The genetically tractable nematode *C. elegans* shares approximately 80% of its genes with humans[25]. The *C. elegans* genome encodes a single homologue of TFEB, the gene *hlh-30* (Supplementary Fig. 7). Its protein product HLH-30 was previously shown to recognize a DNA motif similar to the CLEAR motif *in vitro,* and to drive transcription of metabolic genes *in vivo*[26]. To assess evolutionary conservation of TFEB-mediated starvation responses, we tested whether HLH-30 may act in a similar manner to TFEB during *C. elegans* starvation. First, we found that *hlh-30* mRNA progressively accumulated over a time-course of starvation in wild-type animals, and rapidly decreased after re-introduction of food, similar to mammalian TFEB (Fig. 8a). In contrast, the level of *hlh-30* transcript did not increase after 12h of starvation in *hlh-30(tm1978)* null mutants (Fig. 8b), suggesting that *hlh-30* is induced in an *hlh-30*-dependent manner during starvation by an autoregulatory feedback loop, similar to the mammalian TFEB. *C. elegans* intestinal cells perform similar metabolic functions to the vertebrate liver, including lipid storage and metabolism. Using semi-quantitative Oil Red O staining, we found that starved wild type animals consumed approximately 20% of their lipid stores, compared to well-fed counterparts (Fig. 8c–g). Starved *hlh-30* mutants exhibited a significantly smaller reduction in lipid staining, close to 10%, suggesting that they failed to mobilize lipids as promptly as wild type animals. Consistently, using transmission electron microscopy, we found that intestinal cells in starved wild type animals became depleted of dark-staining lipid droplets (Fig. 8h,i), while those of starved *hlh-30* mutants exhibited abundant droplets (Fig. 8j,k). These results suggest that nematodes, similarly to mice, require HLH-30/TFEB to efficiently use lipid stores during periods of starvation. Furthermore, as in liver TFEB-deficient mice, lipid catabolism gene induction is greatly compromised in starved *hlh-30* mutants (Fig. 8l). These data suggest that the reason starved *hlh-30* mutants fail to mobilize their lipid stores may be because of a severe transcriptional response defect. In wild-type *C. elegans,* starvation results in lifespan extension[27] (Fig. 8m). In contrast, loss of *hlh-30* resulted in almost complete abrogation of starvation-induced lifespan extension (Fig. 8n). Additionally, first stage (L1) wild-type larvae arrest in response to food deprivation, resuming development upon food restoration[28]. In contrast, *hlh-30* mutant L1 larvae completely failed to survive starvation-induced arrest, indicating that *hlh-30* is not only required in adult animals to survive starvation, but in younger stages as well (Fig. 8o). Considered together, these data demonstrate how *hlh-30* expression is induced, that it is required for lipid mobilization, is necessary for a proper transcriptional response, and is required for survival, all during starvation. Therefore, our observations suggest that HLH-30 and murine TFEB share evolutionarily conserved functions in organismal adaptation to starvation.

Discussion

Our study identifies TFEB as a key player in the metabolic response to starvation. TFEB activity is regulated transcriptionally and post-transcriptionally by nutrients, and is required

to induce starvation-response genes in both mammals and worms. Most importantly, the absence of TFEB results in an impairment of lipid catabolism and in a more severe metabolic derangement in obese animals, while TFEB overexpression causes the opposite effects and rescues obesity and associated metabolic syndrome.

TFEB mRNA expression is induced by starvation by a post-transcriptional switch that controls TFEB nuclear translocation[29–31], which allows TFEB to rapidly respond to nutrient availability, and a positive transcriptional autoregulatory component for a sustained response. Autoregulatory feedback circuits are used by eukaryotic cells to convert a graded input into a binary (ON/OFF) response in eukaryotic gene circuits[32–34]. Interestingly, the *PGC1* gene, a direct target of TFEB, is also subject to an autoregulatory loop[35].

Notably, TFEB regulates genes involved in several steps of lipid catabolism, which occur in different cellular compartments, such as the transport of fatty acid chains across the plasma membrane (e.g. *CD36* and *FABPs*), and the oxidation of FFA in mitochondria (e.g. *Cpt1*,*Crat, Acadl Acads, Hdad*) and in peroxisomes (*Cyp4a genes*). According to our data most of the effects of TFEB on lipid metabolism appear to be mediated by the direct regulation exerted by TFEB on the *PGC1 -PPAR* complex. Interestingly, a recent study showed that *PGC1* participates in the transcriptional co-activation of TFEB, although the magnitude of this effect appears to be modest[36].

The observation that TFEB gain and loss of function in the liver influences whole body energy metabolism suggests that TFEB stimulates the liver secretion of factors that affect the function of other tissues. This is likely to be mediated by PGC1 and PPAR , which are known to regulate the production of secreted hormones[37–39].

In previous studies we demonstrated that TFEB controls autophagy by directly regulating lysosomal and autophagy genes[12,13]. Interestingly, the overexpression of *TFEB* in mice in which autophagy was genetically suppressed by deletion of *Atg7* in the liver did not rescue hepatic steatosis, suggesting that TFEB effects on lipid metabolism require a functional autophagic pathway. Thus, TFEB controls the starvation response by orchestrating the induction of autophagy and *PGC1 -PPAR* -mediated lipid catabolism. We propose a model (Supplementary Fig. 8) in which adequate nutrition keeps TFEB inactive by cytoplasmic sequestration. During starvation, TFEB translocates to the nucleus where it induces its own expression. This releases the spring for a fast and dramatic metabolic shift to the catabolism of energy stores. Upon nutrient restoration, the feedback loop is quickly interrupted by TFEB nuclear exclusion, restoring the system to baseline. It is likely that global control of lipid metabolism by TFEB arose early during evolution to facilitate organismal adaptation to challenging nutritional conditions, as evidenced by the evolutionary conservation of TFEB autoregulation and by its role in metabolic adaptation to starvation in the invertebrate C. *elegans*. Finally, the acute beneficial effects of *TFEB* overexpression in both diet- and genetically-induced obese mice suggest that this regulatory circuit may be an attractive therapeutic target for the modulation of lipid metabolism in obesity-related diseases.

Supplementary Material

Refer to Web version on PubMed Central for supplementary material.

Acknowledgments

We thank G. Karsenty, D.Moore, H. Zoghbi, S. Colamarino, E. Abrams, D. Sabatini and R. Zoncu for critical reading of the manuscript. We thank G. Diez-Roux for critical reading of the manuscript, helpful discussions and support in manuscript preparation. We are also grateful to D. Medina, C. Spampanato and F. Annunziata for their

contribution. We acknowledge the support of the Italian Telethon Foundation grant numbers TGM11CB6 (C.S. R. DC., A.B) and TGM11SB1 (A.C, and D.dB), the Beyond Batten Disease Foundation (C.S., F.V., T.H., and A.B.); European Research Council Advanced Investigator grant no. 250154 (A.B.); March of Dimes #6-FY11-306 (A.B); US National Institutes of Health (R01-NS078072) (A.B). This work was supported in part by grants from the US National Institutes of Health (R01-HL51586) to L.C. and the Diabetes and Endocrinology Research Center (P30-DK079638, L.C.) and the Mouse Metabolism Core (P.K.S) at Baylor College of Medicine. TJK is in part supported by the Cancer Prevention and Research Institute of Texas (RP110390). O. V. was funded by a Fund for Medical Discovery postdoctoral fellowship from the Massachusetts General Hospital. This study was funded in part by the National Institute of General Medical Sciences of the National Institutes of Health under award number R01GM101056-01 to J. E. I. The content is solely the responsibility of the authors and does not necessarily represent the official views of the National Institutes of Health

References

1. Bauer M, et al. Starvation response in mouse liver shows strong correlation with lifespan-prolonging processes. Physiol Genomics. 2004; 17:230–244. [PubMed: 14762175]
2. Sokolovic M, et al. The transcriptomic signature of fasting murine liver. BMC Genomics. 2008; 9:528. [PubMed: 18990241]
3. Hakvoort TB, et al. Interorgan coordination of the murine adaptive response to fasting. J Biol Chem. 2011; 286:16332–16343. [PubMed: 21393243]
4. Finn PF, Dice JF. Proteolytic and lipolytic responses to starvation. Nutrition. 2006; 22:830–844. [PubMed: 16815497]
5. Fontana L, Partridge L, Longo VD. Extending healthy life span--from yeast to humans. Science. 2010; 328:321–326. [PubMed: 20395504]
6. Zinke I, Schutz CS, Katzenberger JD, Bauer M, Pankratz MJ. Nutrient control of gene expression in Drosophila: microarray analysis of starvation and sugar-dependent response. The EMBO journal. 2002; 21:6162–6173. [PubMed: 12426388]
7. Van Gilst MR, Hadjivassiliou H, Yamamoto KR. A Caenorhabditis elegans nutrient response system partially dependent on nuclear receptor NHR-49. Proc Natl Acad Sci U S A. 2005; 102:13496–13501. [PubMed: 16157872]
8. Mizushima N. Autophagy: process and function. Genes Dev. 2007; 21:2861–2873. [PubMed: 18006683]
9. Singh R, et al. Autophagy regulates lipid metabolism. Nature. 2009; 458:1131–1135. [PubMed: 19339967]
10. Singh R, Cuervo AM. Autophagy in the cellular energetic balance. Cell Metab. 2011; 13:495–504. [PubMed: 21531332]
11. Yang L, Li P, Fu S, Calay ES, Hotamisligil GS. Defective hepatic autophagy in obesity promotes ER stress and causes insulin resistance. Cell Metab. 2010; 11:467–478. [PubMed: 20519119]
12. Sardiello M, et al. A gene network regulating lysosomal biogenesis and function. Science. 2009; 325:473–477. [PubMed: 19556463]
13. Settembre C, et al. TFEB links autophagy to lysosomal biogenesis. Science. 2011; 332:1429–1433. [PubMed: 21617040]
14. Palmieri M, et al. Characterization of the CLEAR network reveals an integrated control of cellular clearance pathways. Hum Mol Genet. 2011; 20:3852–3866. [PubMed: 21752829]
15. Dennis G Jr, et al. Database for Annotation, Visualization, and Integrated Discovery. Genome Biol. 2003; 4:P3. [PubMed: 12734009]
16. Huang da W, Sherman BT, Lempicki RA. Systematic and integrative analysis of large gene lists using DAVID bioinformatics resources. Nat Protoc. 2009; 4:44–57. [PubMed: 19131956]
17. Finck BN, Kelly DP. PGC-1 coactivators: inducible regulators of energy metabolism in health and disease. J Clin Invest. 2006; 116:615–622. [PubMed: 16511594]
18. Spiegelman BM, Heinrich R. Biological control through regulated transcriptional coactivators. Cell. 2004; 119:157–167. [PubMed: 15479634]
19. Vega RB, Huss JM, Kelly DP. The coactivator PGC-1 cooperates with peroxisome proliferator-activated receptor alpha in transcriptional control of nuclear genes encoding mitochondrial fatty acid oxidation enzymes. Mol Cell Biol. 2000; 20:1868–1876. [PubMed: 10669761]

20. Lin J, Handschin C, Spiegelman BM. Metabolic control through the PGC-1 family of transcription coactivators. Cell Metab. 2005; 1:361–370. [PubMed: 16054085]
21. Komatsu M, et al. Impairment of starvation-induced and constitutive autophagy in Atg7-deficient mice. J Cell Biol. 2005; 169:425–434. [PubMed: 15866887]
22. Komatsu M, et al. Homeostatic levels of p62 control cytoplasmic inclusion body formation in autophagy-deficient mice. Cell. 2007; 131:1149–1163. [PubMed: 18083104]
23. Bordone L, et al. SIRT1 transgenic mice show phenotypes resembling calorie restriction. Aging Cell. 2007; 6:759–767. [PubMed: 17877786]
24. Vaisse C, et al. Leptin activation of Stat3 in the hypothalamus of wild-type and ob/ob mice but not db/db mice. Nat Genet. 1996; 14:95–97. [PubMed: 8782827]
25. Lai CH, Chou CY, Ch'ang LY, Liu CS, Lin W. Identification of novel human genes evolutionarily conserved in Caenorhabditis elegans by comparative proteomics. Genome Res. 2000; 10:703–713. [PubMed: 10810093]
26. Grove CA, et al. A multiparameter network reveals extensive divergence between C. elegans bHLH transcription factors. Cell. 2009; 138:314–327. [PubMed: 19632181]
27. Kaeberlein TL, et al. Lifespan extension in Caenorhabditis elegans by complete removal of food. Aging Cell. 2006; 5:487–494. [PubMed: 17081160]
28. Johnson TE, Mitchell DH, Kline S, Kemal R, Foy J. Arresting development arrests aging in the nematode Caenorhabditis elegans. Mech Ageing Dev. 1984; 28:23–40. [PubMed: 6542614]
29. Settembre C, et al. A lysosome-to-nucleus signalling mechanism senses and regulates the lysosome via mTOR and TFEB. EMBO J. 201210.1038/emboj.2012.32
30. Martina JA, Chen Y, Gucek M, Puertollano R. MTORC1 functions as a transcriptional regulator of autophagy by preventing nuclear transport of TFEB. Autophagy. 2012; 8
31. Roczniak-Ferguson A, et al. The Transcription Factor TFEB Links mTORC1 Signaling to Transcriptional Control of Lysosome Homeostasis. Sci Signal. 2012; 5:ra42. [PubMed: 22692423]
32. Becskei A, Seraphin B, Serrano L. Positive feedback in eukaryotic gene networks: cell differentiation by graded to binary response conversion. The EMBO journal. 2001; 20:2528–2535. [PubMed: 11350942]
33. Siciliano V, et al. Construction and modelling of an inducible positive feedback loop stably integrated in a mammalian cell-line. PLoS Comput Biol. 2011; 7:e1002074. [PubMed: 21765813]
34. Kielbasa SM, Vingron M. Transcriptional autoregulatory loops are highly conserved in vertebrate evolution. PLoS One. 2008; 3:e3210. [PubMed: 18791639]
35. Handschin C, Rhee J, Lin J, Tarr PT, Spiegelman BM. An autoregulatory loop controls peroxisome proliferator-activated receptor gamma coactivator 1alpha expression in muscle. Proc Natl Acad Sci U S A. 2003; 100:7111–7116. [PubMed: 12764228]
36. Tsunemi T, et al. PGC-1alpha rescues Huntington's disease proteotoxicity by preventing oxidative stress and promoting TFEB function. Sci Transl Med. 2012; 4:142ra197.
37. Bostrom P, et al. A PGC1-alpha-dependent myokine that drives brown-fat-like development of white fat and thermogenesis. Nature. 2012; 481:463–468. [PubMed: 22237023]
38. Badman MK, et al. Hepatic fibroblast growth factor 21 is regulated by PPARalpha and is a key mediator of hepatic lipid metabolism in ketotic states. Cell Metab. 2007; 5:426–437. [PubMed: 17550778]
39. Inagaki T, et al. Endocrine regulation of the fasting response by PPARalpha-mediated induction of fibroblast growth factor 21. Cell Metab. 2007; 5:415–425. [PubMed: 17550777]

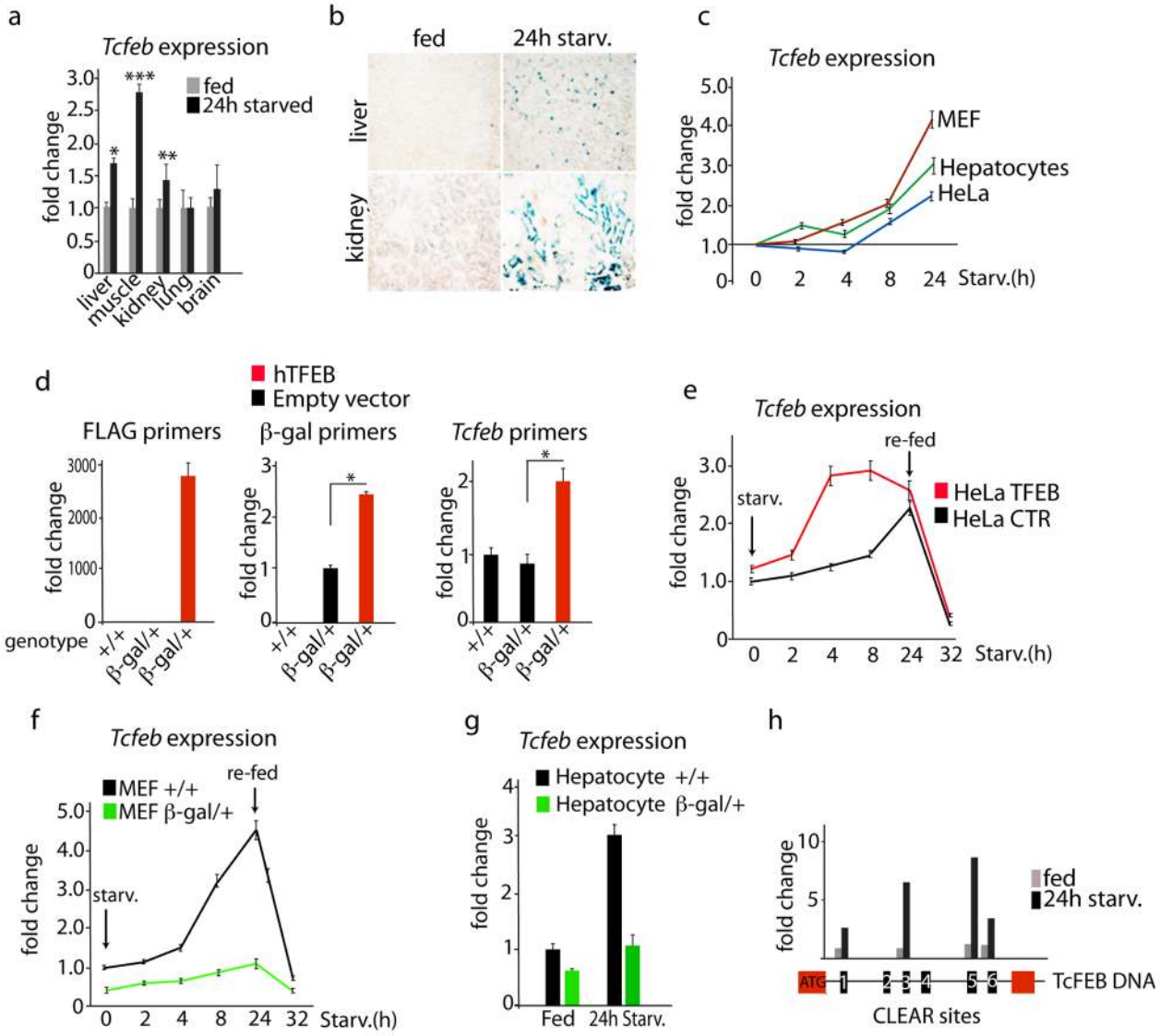

Fig. 1. Autoregulation of TFEB during starvation

a) Expression levels of *Tcfeb* mRNA in tissues isolated from 24h-fasted (starv) 6 week old mice. Values are expressed as fold change relative to *Tcfeb* expression in mice fed *ad libitum* (fed). Bars represent mean±s.d. for n=5; *P ≤0.05; **P ≤0.01; ***P ≤0.001. **b**) Representative βgal staining of liver and kidney frozen sections isolated from fed and 24h–fasted heterozygous *Tcfeb*- βgal mice. **c)** Time-course expression analysis of *TFEB* in wild-type HeLa cells, MEFs and hepatocytes after addition of starvation media (time 0). Bars represent mean±s.d. for n=3 independent experiments. **d)** Expression levels of transfected hTFEB-Flag, *Tcfeb*- βgal fusion transcript and endogenous *Tcfeb* mRNAs in MEFs isolated from control (+/+) and heterozygous *Tcfeb*- βgal/+ mice. Bars represent mean±s.d. for n=3 **e)** Time-course expression analysis of *TFEB* mRNA in control or *TFEB*-overexpressing HeLa cells during fasting and re-feeding. Primers specific for the endogenous *TFEB* were used. Bars represent mean±s.d. for n=3 **f)** Time-course expression analysis of *Tcfeb* mRNA in heterozygous *Tcfeb*- βgal/+ or control MEFs during fasting and re-feeding. Specific primers for the endogenous *Tcfeb* were used. Bars represent mean±s.d. for n=3 **g)** Expression analysis of *Tcfeb* mRNA in heterozygous Tcfeb- βgal/+ or control hepatocytes

in fed and after 24h fasting. Bars represent mean±s.d. for n=3 **h)** Chromatin immunoprecipitation (ChIP) analysis from liver of mice fed *ad libitum* or 24h-fasted. The CLEAR elements in the first intron of *Tcfeb* genomic DNA are shown as numbered black boxes as indicated in Supplementary Table 1. Red boxes represent exons, and the ATG indicates the first codon (from the mouse *Tcfeb* isoform b). The histogram shows the amount of immunoprecipitated DNA as detected by qPCR assay. Values were normalized to the input and plotted as relative enrichment over a mock control. Data represent mean ± s.d of three independent experiments.

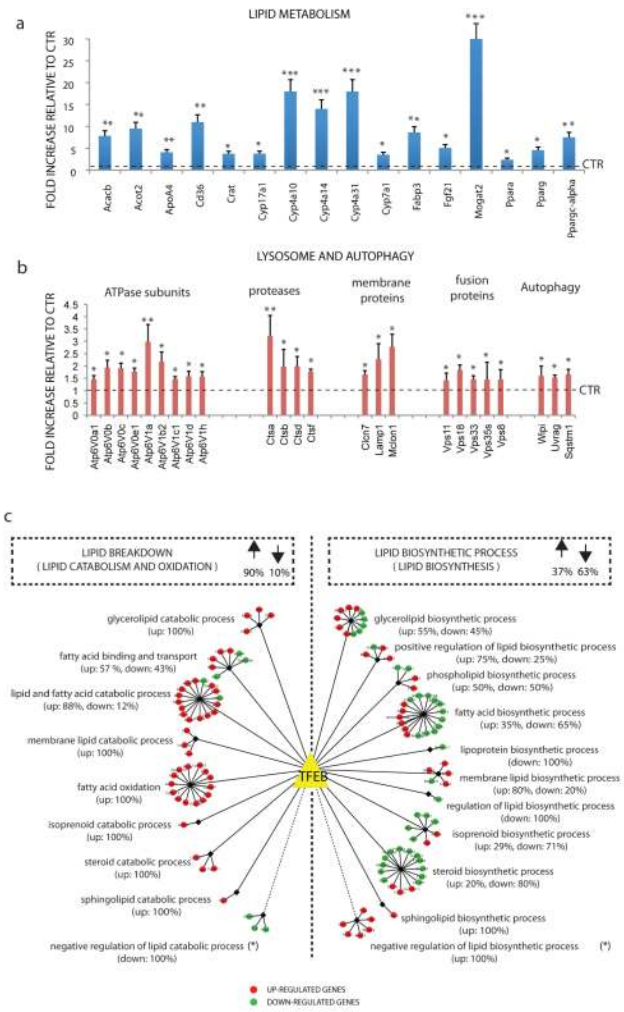

Fig. 2. The TFEB lipid metabolism network

a, b) mRNA levels of the indicated genes involved in (**a**) lipid metabolism and in (**b**) autophagy and lysosome pathway were quantified by qRT–PCR in total RNA isolated from liver samples of mice infected with HDAd-TFEB virus. GAPDH was used as a control. Values are mean± s.d for n=3 and are expressed as fold increase compared to control mice (injected with transgeneless viral vector). * $p<0.05$; **<0.01. Control levels are indicated by dashed line. **c**) The 124 genes with a known role in the lipid metabolic process, whose expression was perturbed by *TFEB* overexpression, are represented as coloured circles and assigned to specific lipid breakdown (left) or lipid biosynthesis (right) sub-categories. The percentages of up-regulated (red circles) and down-regulated genes (green circles) are shown both for the two main groups and for each sub-category. *Note that in calculating these percentages genes assigned to the “negative” regulation of lipid catabolic process and to the “negative” regulation of lipid biosynthetic process have been included in the lipid breakdown and in the lipid biosynthesis groups, respectively.

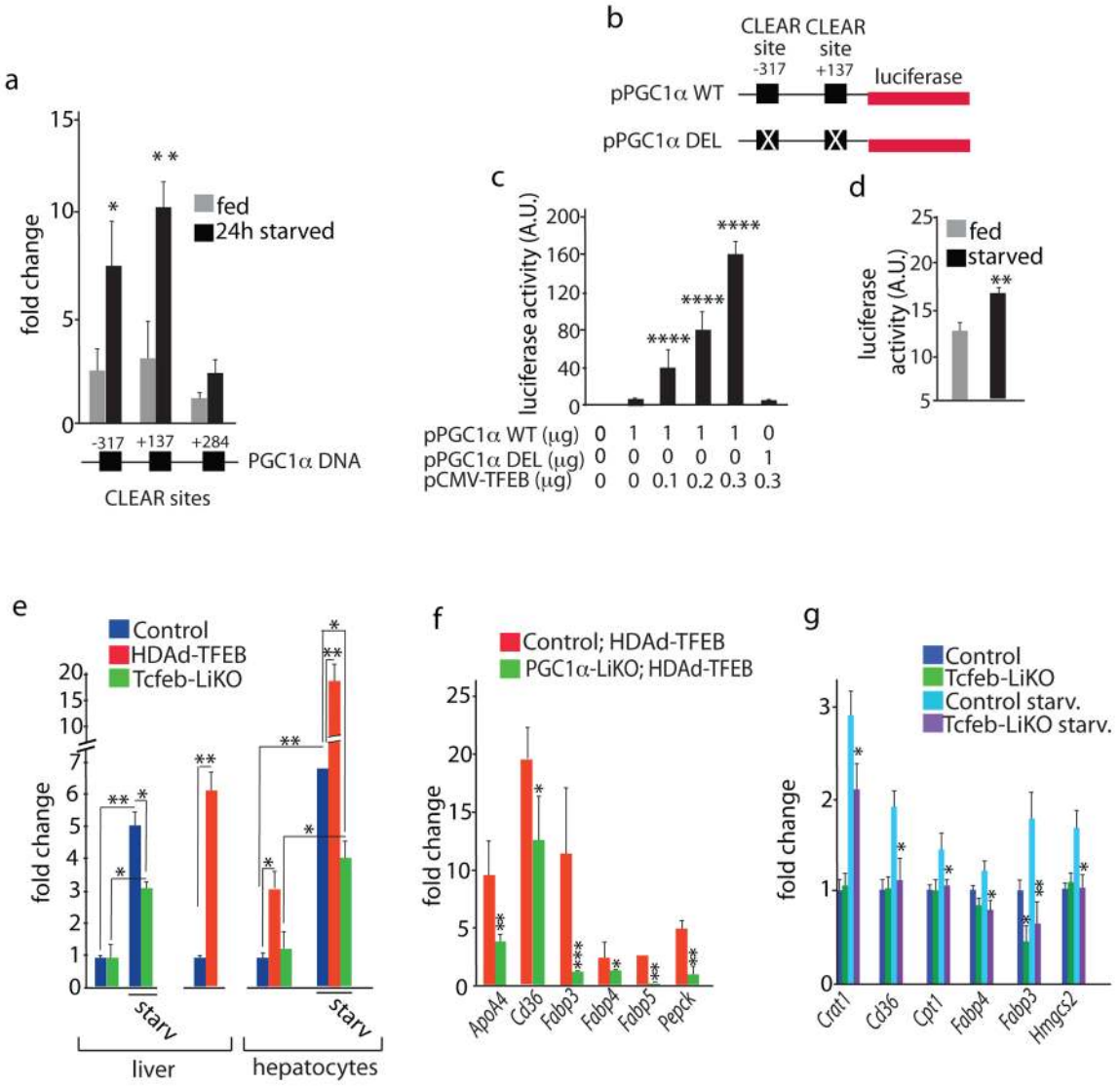

Fig. 3. TFEB directly regulates *PGC1 α* expression during starvation

a) Chromatin immunoprecipitation (ChIP) analysis from liver of mice fed *ad libitum* (fed) or 24h-fasted (starved). CLEAR sites in the promoter region of *PGC1 α* are indicated by boxes. Numbers indicate the distance (bp) of the binding element from the start codon. Bar graphs show the amount of immunoprecipitated DNA as detected by qPCR assay. Values were normalized to the input and plotted as relative enrichment over a mock control. Bar graphs represent mean ± s.d of 3 independent experiments *P ≤0.05; **P ≤0.01. **b)** Representative diagrams of the constructs containing the promoter region of *PGC1 α* with either intact (PGC1 αWT) or deleted (PGC1 αDEL) CLEAR elements upstream of the luciferase cDNA. **c)** Luciferase activity was measured after transfecting increasing amounts of TFEB-Flag in combination with PGC1 αWT or PGC1 αDEL plasmids. Bar graphs represent mean ± s.d. of n=3 independent experiments *P ≤0.05; **P ≤0.01; ****P ≤0.0001 compared to mock transfected cells.**d)** Luciferase activity was measured in cells stably overexpressing TFEB cultured in normal and starved media. Bar graphs represent mean ± s.d. of n=3 independent experiments *P ≤0.05; **P ≤0.01; ****P ≤0.0001 compared to mock transfected cells. **e)** Quantification of mRNA levels of PGC1 αin liver and hepatocytes from control, HDAd-

TFEB and *Tcfeb*-LI^{KO} mice treated as indicated. Bar graphs show mean ±s.d. for n=4. *P ≤0.05; **P ≤0.01; ***P ≤0.001. **f)** Expression analysis of TFEB target genes in liver of mice with indicated genotypes. Bar graphs show mean ±s.d. for n=3. *P ≤0.05; **P ≤0.01; ***P ≤0.001. **g)** Expression analysis of PGC1 /PPAR target genes in liver from either fasted or fed mice with indicated genotypes. Bar graphs show mean ±s.d. for n=4. *P ≤0.05; **P ≤0.01; ***P ≤0.001 compared to the respective controls (fed or fasted).

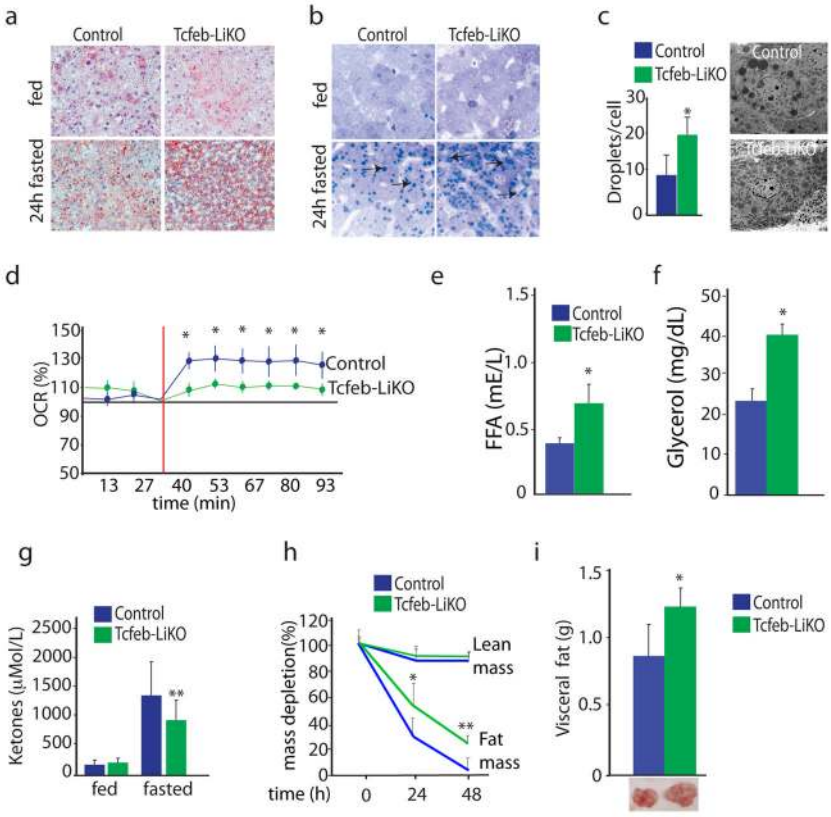

Fig. 4. Liver fat catabolism in response to starvation is regulated by TFEB

a) Oil red O staining of liver sections isolated from mice with the indicated genotype fed *ad libitum* and 24h-fasted. Original magnication 40X. **b)** Toluidin blue staining of liver sections isolated from fed and 24-h–fasted Tcfeb-LiKO and control mice (Tcfeb flox/flox mice). Arrows indicate lipid droplets. Original magnication 100x. **c)** Bar graphs show the quantification of the number of lipid droplets/hepatocyte from electron microscopy analysis. Representative image is showed on the right. Values are mean±s.d. of at least 10 cell/mice (n=3 mice/group). *P ≤0.05; ***P ≤0.001 **d)** Oxygen consumption rate in primary hepatocytes isolated from control and Tcfeb-LiKO mice was measured with an XF24 analyzer (Seahorse) prior and after addition of palmitic acid (0.2 mM) conjugated with BSA. The vertical red line indicates the time at which palmitate was added to cells. Values are mean±s.d. for 3 independent experiments *P ≤0.05. **e)** Total FFA and **f)** glycerol in the serum isolated from 6h fasted Tcfeb-LiKO and control mice. Values are mean ± s.d. (n= 5) *P ≤0.05; **P ≤0.01; ****P ≤0.0001 compared to controls. **g)** Total serum ketones in fed and fasted Tcfeb-LiKO and control mice. Bars are mean±s.d. for n=10. *P ≤0.05; **P ≤0.01 compared to fed control mice. **h)** EchoMRI measurement of fat and lean mass in fed and in 24-h and 48-h fasted mice expressed as relative % to fed (100% in the graph). Indicated values are mean±s.d. for n=5. *P ≤0.05; **P ≤0.01 compared to fed control mice. **i)** Visceral fat pad mass isolated from 2-month-old-mice with indicated genotypes. Indicated values are mean± s.d. for n=5. *P ≤0.05; compared to fed control mice.

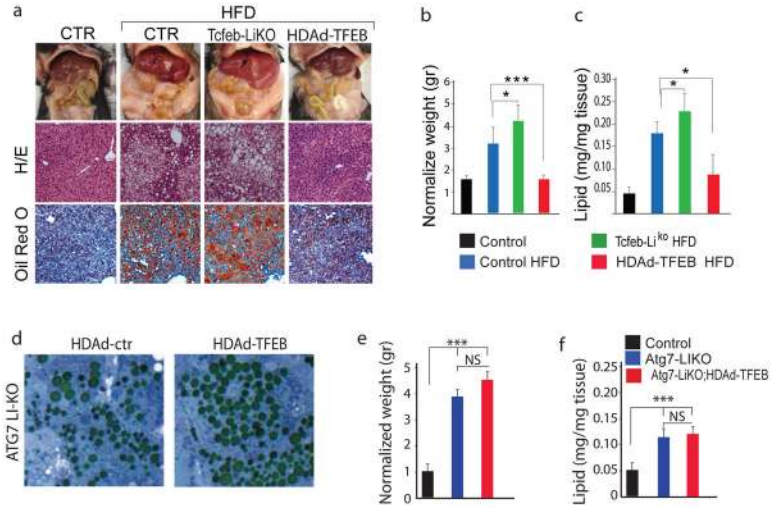

Fig. 5. TFEB regulates lipid catabolism through the autophagic pathway

a) Mice with indicated genotype were kept on a high-fat diet for 12 weeks when indicated (HFD). Gross liver morphology (upper panel), H/E (middle panel), and oil red O staining of liver sections (bottom panel). **b)** Bar graph shows normalized liver weights (mean±s.d. for n=10) and **c)** total lipid content in mice with indicated genotype (mean±s.d. for n=10). *P ≤0.05; **P ≤0.01; ***P ≤0.001 compared to control. **d)** Toluidin blue staining of liver sections isolated from ATG7KO mice injected with HDAd-ctr or HDAd-TFEB vector. **e)** Bar graph shows normalized liver weights (mean±s.d. for n=10 ***P ≤0.001) and **f)** total lipid content in mice with indicated genotype (mean±s.d. for n=5; ***P ≤0.001). Mice injected with an empty HDAd virus behaved as wild-type untreated mice, therefore data is not represented in the figure.

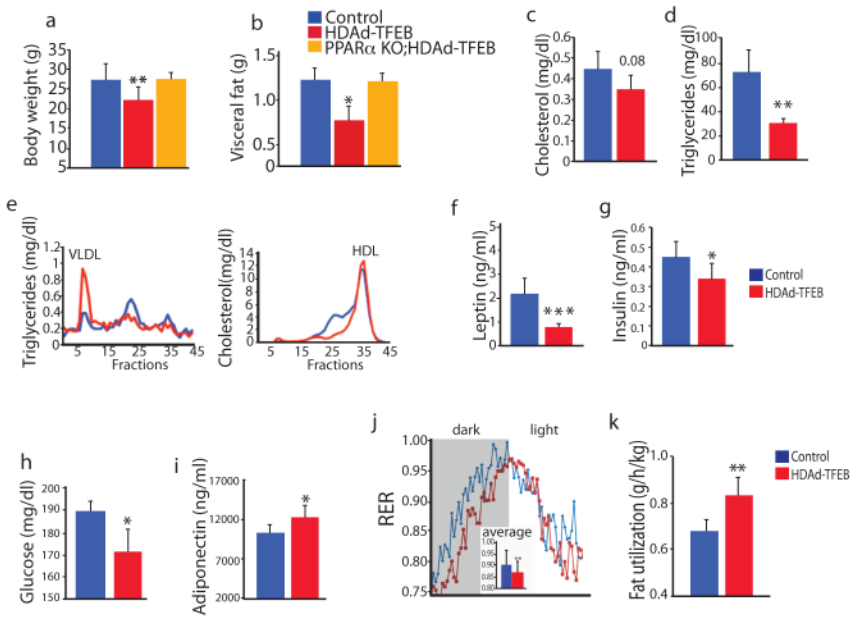

Fig. 6. Metabolic profile of HDAd-TFEB overexpressing mice

(a) Body weight and **(b)** visceral fat mass isolated from 2-month-old-mice with the indicated genotypes. n=5. **(c–i)** Serum metabolic profile in HDad-TFEB mice compared to control mice. **(j)** Respiratory exchange ratio (RER; VCO2/VO2) and **(k)** fatty acid utilization calculated from data in **(j)**. Values are mean ± s.d (n = 10) *P_0.05; **P_0.01; compared to controls.

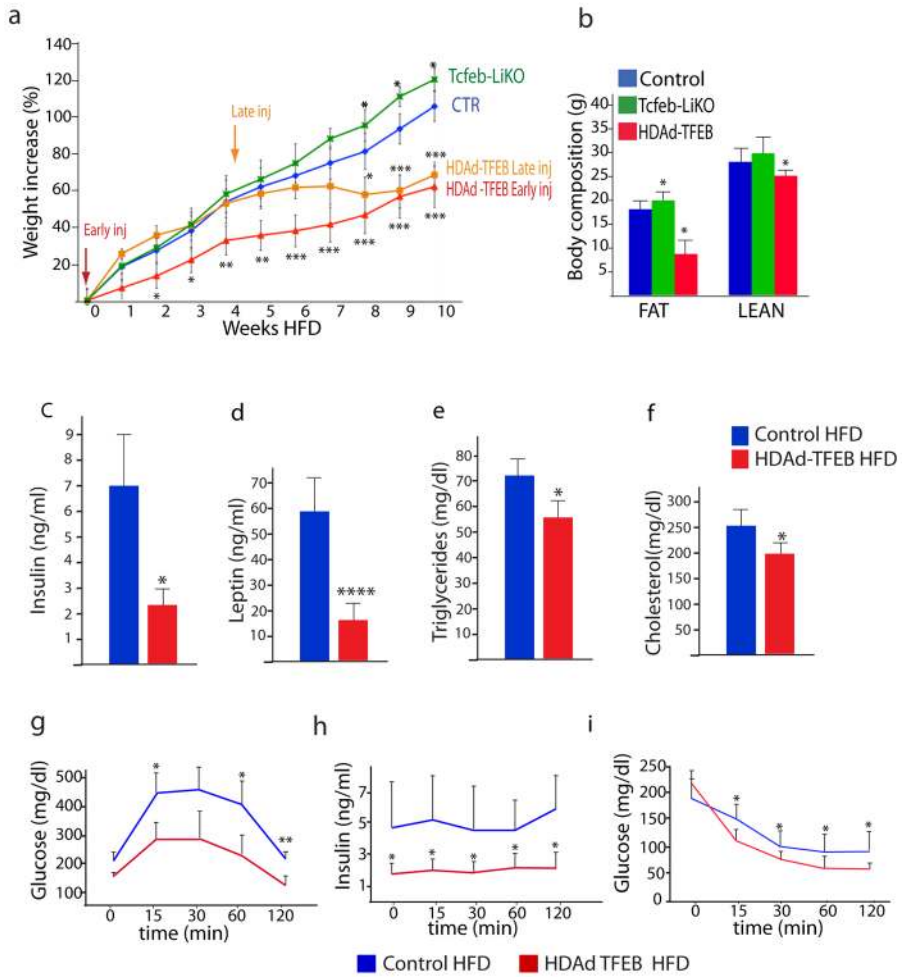

Fig. 7. TFEB prevents diet-induced obesity and metabolic syndrome

a) Body weight curves of male mice fed with HFD (40% calories from fat) for 10 weeks starting from 5 weeks of age (0 on the x axes). Mice were injected with HDAd-*TFEB* either 1week before (early inj.), or 4 weeks after, (late inj.) being placed on the HFD, as indicated by the arrows. Values are represented as percentages of weight increase. **b)** Whole body composition analysis (Echo MRI) of the same mice as in (**a**) after 10 weeks of HFD. In **a** and **b** n=10 mice/group; bars represent mean±s.d. *P ≤0.05; **P ≤0.01; ***P ≤0.001 compared to control HFD group. **c–f)** Total serum insulin, leptin, triglyceride and cholesterol levels in control and HDAd-*TFEB* mice kept on high-fat diet (HFD) for 10 weeks. Value are mean ±s.d. n=10. *P ≤0.05; ****P ≤0.0001 compared to control. **g–i)** Glucose and insulin tolerance tests in control and HDAd-*TFEB* mice challenged with HFD for 10 weeks. (**g**) Glucose and (**h**) serum insulin levels at the indicated time points after glucose challenge. (**i**) Glucose levels at the indicated time points after insulin challenge. In **g**,**h**,**i** value are mean ±s.d. n=7 mice/group; *P ≤0.05; **P ≤0.01; ***P ≤0.001 compared to control. Mice injected with an empty HDAd virus behaved as wild-type untreated mice, therefore data is not represented in the figure.

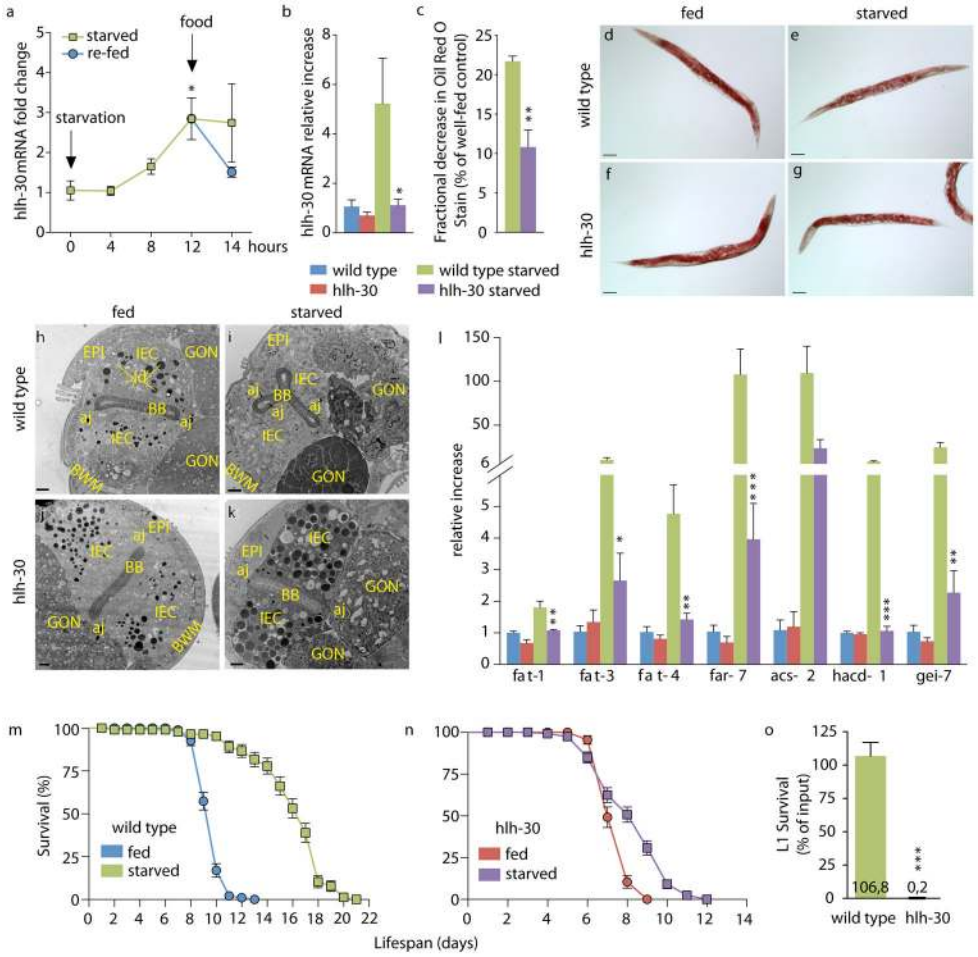

Fig. 8. Conservation of TFEB-mediated autoregulation and of starvation response in *C. elegans*.

a) *hlh-30* qRT-PCR showing increased expression of *C. elegans* TFEB gene *hlh-30* over a time course of starvation in wild type animals followed by a rapid decrease to basal level following re-feeding of the animals (mean ± s.e.m. of n=3). *P ≤0.05 (*t* test, compared with wild type at t = 0 h). **b)** *hlh-30* 3 □UTR qRT-PCR showing expression of *hlh-30* after 12 h starvation in wild type and *hlh-30(tm1978)* animals (mean ± s.e.m. of n=3). *P ≤0.05 (*t* test, compared with wild type starved). **c**) Quantification of oil red O stain in starved animals relative to well-fed counterparts (mean ± s.e.m. of n=3).**P ≤0.01 (*t* test, compared with wild type starved). **d–g)** Representative micrographs of wild type and *hlh-30* animals after 8 h starvation and stained with oil red O. **h–k)** Representative TEMs of wild type and *hlh-30* animals after 24 h starvation. IEC, intestinal epithelial cell; EPI, epidermis; BB, brush border; GON, gonad; BWM, body wall muscles, aj, apical junction; ld, lipid droplet. Scale bar is 2 □m. **l)** qRT-PCR of starvation-induced genes in wild type and *hlh-30* animals after 12 h starvation (means ± s.e.m of n=3). *P ≤0.05; **P ≤0.01; ***P ≤0.001 (*t* test, compared with wild type starved). **m–n)** *hlh-30* is required for starvation-induced lifespan extension. One representative experiment of two independent trials; error bars represents mean ± s.e.m. Median Survival (MS) (wild type fed) = 10 d; MS (wild type starved) = 17 d, P < 0.0001 vs fed using the Log-rank test; MS (*hlh-30* fed) = 7 d; MS (*hlh-30* starved) = 9 d, P < 0.0001 vs fed. **o**) L1 arrest assay showing survival of wild-type and *hlh-30* starved animals relative to non-starved conditions (mean ± s.e.m. of n=3). ***P ≤0.001 (*t* test, compared with wild type starved).